JOURNAL OF GEOPHYSICAL RESEARCH, VOL. 105, NO. B9, PAGES 21,529–21,536, SEPTEMBER 10, 2000

Conditions for compaction bands in porous rock

K. A. Issen[1] and J. W. Rudnicki
Department of Civil Engineering, Northwestern University, Evanston, Illinois

Abstract. Reexamination of the results of Rudnicki and Rice for shear localization reveals that solutions for compaction bands are possible in a range of parameters typical of porous rock. Compaction bands are narrow planar zones of localized compressive deformation perpendicular to the maximum compressive stress, which have been observed in high-porosity rocks in the laboratory and field. Solutions for compaction bands, as an alternative to homogenous deformation, are possible when the inelastic volume deformation is compactive and is associated with stress states on a yield surface "cap." The cap implies that the shear stress required for further inelastic deformation decreases with increasing compressive mean stress. While the expressions for the critical hardening modulus for compaction and shear bands differ, in both cases, deviations from normality promote band formation. Inelastic compaction deformation associated with mean stress (suggested by Aydin and Johnson) promotes localization by decreasing the magnitude of the critical hardening modulus. Axisymmetric compression is the most favorable deviatoric stress state for formation of compaction bands. Predictions for compaction bands suggest that they could form on the "shelf" typically observed in axisymmetric compression stress strain curves of porous rock at high confining stress. Either shear or compaction bands may occur depending on the stress path and confining stress. If the increase in local density and decrease in grain size associated with compaction band formation result in strengthening rather than weakening of the band material, formation of a compaction band may not preclude later formation of a shear band.

1. Introduction

Mollema and Antonelli [1996] recently identified localized deformation structures in high porosity sandstone, which they referred to as "compaction bands." These bands consisted of thin tabular zones of pure compressional deformation that were characterized by a significant reduction in porosity (from 20-25% to a few percent). Owing to reduced permeability, these compaction bands could trap hydrocarbons and act as barriers to fluid flow in otherwise more permeable rock. The compaction bands were often found near the tips of localized shear bands, suggesting that the formation of these two band types may be related.

Olsson [1999] discussed these field observations and experimental evidence of compaction bands associated with artificial shear cracks and stressed boreholes. In addition, he conducted axisymmetric compression tests on Castlegate sandstone (25-30% porosity). Several specimens exhibited zones of localized compaction perpendicular to the direction of maximum compressive stress, which he interpreted as compaction bands. Shear bands, with band normal orientations ranging from 14° to 43° to the maximum compressive stress, were observed in some specimens. All specimens exhibited compaction bands, shear bands, or both. To explain the origin of compaction bands, *Olsson* [1999] recognized that the approach of *Rudnicki and Rice* [1975], used to predict the occurrence of shear bands, could be applied. In particular, he noted that for a special combination of material parameters, which could be appropriate for compacting rock, the theory predicts a planar band perpendicular to the most compressive principal stress, as expected for a compaction band.

In this paper, we extend the theoretical considerations of *Olsson* [1999]. More specifically, we show that the results of *Rudnicki and Rice* [1975] admit compaction bands, that is, bands of localized deformation perpendicular to the maximum compressive stress, not just for the particular case identified by *Olsson* [1999] but for a range of material parameters. *Rudnicki and Rice* [1975] actually noted this possibility but dismissed it because the required values of material parameters were inappropriate for the low-porosity, dilatant rock on which they focused. As *Olsson* [1999] points out and we discuss here, values of material parameters appropriate for high-porosity, compacting rock can lie in the range for which compaction bands are predicted. Here we discuss the predictions for compaction bands within the *Rudnicki and Rice* [1975] theory and their relation to predictions of shear bands.

[1]Now at Department of Mechanical and Aeronautical Engineering, Clarkson University, Potsdam, New York.

Paper number 2000JB900185.
0148-0227/00/2000JB900185$09.00

2. Review of Localization Theory

Building upon earlier work by *Hadamard* [1903], *Thomas* [1961], *Hill* [1962], and *Mandel* [1966], *Rudnicki and Rice* [1975] (herein referred to as RR) attempted to model the onset of localized deformation as a nonuniqueness or bifurcation from homogeneous deformation. That is, for boundary conditions for which continued homogeneous deformation is a solution, they consider the possibility that another solution, corresponding to localized deformation in a planar band with normal n_i, is possible. Band formation is subject to conditions of kinematic compatibility and stress equilibrium.

The kinematic condition results from the requirement that the velocity field be continuous at the inception of nonuniqueness and that velocity gradients vary only with position across the band and vanish in the homogeneous field outside it:

$$\Delta(v_{i,j}) = n_j g_i(\mathbf{n}\cdot\mathbf{x}), \tag{1}$$

where v_i is the velocity, $v_{i,j} = \partial v_i/\partial x_j$, and Δ denotes the difference between the local field inside the band and the uniform field outside. The g_i are functions of distance across the band, and are non-zero only within the band. For a shear band with no compaction or dilation, the difference between the velocity gradient field inside and outside the band is simple shear and $\mathbf{n}\cdot\mathbf{g} = 0$. For the materials considered by RR, dilation accompanies inelastic shear strain. Consequently, $\mathbf{n}\cdot\mathbf{g} \neq 0$, and the difference field is a combination of simple shear and uniaxial dilation normal to the band. Similarly, for materials that compact upon inelastic shearing the difference field is a combination of simple shear and uniaxial compression normal to the band. *Olsson* [1999] noted, however, that it is possible to seek a solution corresponding to the observations of *Mollema and Antonelli* [1996], for which the difference field is pure compression normal to the band, and thus $\mathbf{g}$ is in the direction of $\mathbf{n}$. These results are discussed in more detail by P. Bésuelle (Compacting and dilating shear bands in porous rock: theroretical and experimental conditions, submitted to *J. Geophys. Res.*, 2000), who identifies the smooth transition from pure dilation bands to pure compaction bands, via shear bands which evolve from dilating to compacting.

Formation of the band must also satisfy conditions of continuing equilibrium. This requires that the traction rates be continuous across the band boundary:

$$n_i \Delta\dot{\sigma}_{ij} = 0, \tag{2}$$

where σ_{ij} is the (Cauchy) stress and the over dot denotes its rate.

The remaining ingredient needed to complete the formulation is the constitutive relation. A large class of rate-independent constitutive relations can be written in the following form:

$$\dot{\sigma}_{ij} = L_{ijkl} D_{kl}, \tag{3}$$

where $D_{ij} = \frac{1}{2}(v_{i,j} + v_{j,i})$ is the deformation rate and L_{ijkl} is the modulus tensor. (To be rigorous, the rate in (3) should be a corotational rate, invariant to rigid body spins, but the consequences of neglecting this difference in what follows are small and discussed in more detail by RR.) In the simplest case, the material inside and outside of the band behaves identically at the instant of band formation. (*Rice and Rudnicki* [1980] have shown that for the constitutive relation considered by RR, band formation with elastic unloading outside the band cannot precede formation with both the material inside and outside of the band loading nonelastically.) Combining (1), (2), and (3) yields

$$(n_i L_{ijkl} n_l) g_k = 0. \tag{4}$$

Further homogeneous deformation, corresponding to $g_k = 0$, is one possible solution, but an alternative solution, corresponding to band formation, is possible when at least one of the g_k is nonzero. This requires that the determinant of the coefficients in (4) vanish:

$$\det|n_i L_{ijkl} n_l| = 0. \tag{5}$$

This condition constrains the orientation of the band and the values of the constitutive parameters. Band formation is predicted to occur when this condition is first met in a program of deformation.

3. Constitutive Relations

The constitutive relation used by RR to describe features of brittle rock deformation has the following form for the simple stress state combining pure shear τ and hydrostatic compression σ:

$$d\gamma = \frac{d\tau}{G} + \frac{1}{h}(d\tau - \mu d\sigma) \tag{6}$$

$$d\varepsilon = -\frac{d\sigma}{K} + \frac{\beta}{h}(d\tau - \mu d\sigma), \tag{7}$$

where $d\gamma$ and $d\varepsilon$ are increments of shear strain and volume strain. The first terms are elastic contributions with shear modulus G and bulk modulus K; the second terms are inelastic and are omitted for elastic unloading. Inelastic shear strain is inhibited by hydrostatic compression, and $\mu = d\tau/d\sigma$ is the local slope of the yield surface in stress space, dividing regions of elastic unloading from regions of further inelastic response. The ratio of increments of inelastic volume strain to inelastic increments of shear strain is β:

$$d^p\varepsilon = \beta d^p\gamma. \tag{8}$$

Thus β is a dilation coefficient, positive for dilation, negative for compaction. The slope of the τ versus. γ curve at constant mean stress (σ) is given by $h_{\tan} = h/(1 + h/G)$, where the hardening modulus h is the slope of the τ versus. γ^p curve at constant mean stress.

Rudnicki and Rice [1975] generalized the relations (6) and (7) to arbitrary stress states by assuming isotropic elasticity, replacing σ by the mean normal stress, $-\frac{1}{3}\sigma_{kk}$ (σ_{kk} positive in tension) and the shear stress τ by the Mises equivalent stress $\bar{\tau} = \sqrt{\frac{1}{2}s_{ij}s_{ij}}$, where $s_{ij} = \sigma_{ij} - \frac{1}{3}\delta_{ij}\sigma_{kk}$ is the deviatoric stress, δ_{ij} ($= 1$ if $i = j$ and $= 0$ if $i \neq j$) is the Kronecker delta, and repeated subscripts imply summation. When this is done, the modulus tensor in (3) is given by

$$L_{ijkl} = G(\delta_{ik}\delta_{jl} + \delta_{il}\delta_{jk}) + (K - \frac{2}{3}G)\delta_{ij}\delta_{kl} - \frac{(GN_{ij} + \beta K\delta_{ij})(GN_{kl} + \mu K\delta_{kl})}{h + G + \mu\beta K}, \quad (9)$$

where $N_{ij} = s_{ij}/\bar{\tau}$.

RR focused on low-porosity rock, for which inelastic response is dilatant; inelastic shear strain causes inelastic volume increase. However, compressed high-porosity rock typically experiences initial compaction, followed by either dilation or further compaction, depending upon the stress state [*Wong et al.*, 1997]. For Castlegate sandstone, *Olsson* [1999] reports negative values for the dilatancy factor β and moderately positive to slightly negative values for the friction coefficient μ. The slope of the yield surface in the $\bar{\tau}$ versus. σ plane will necessarily be negative if the surface is closed on the hydrostatic axis, or has a "cap," and, by symmetry, will become unbounded in magnitude as the hydrostatic axis is approached. A particular example identified by *Wong et al.* [1992] and referenced by *Olsson* [1999] is the two-yield surface model, similar to that suggested by *DiMaggio and Sandler* [1971] for granular soils: a shear yield surface (similar to RR, $\mu > 0$), with a cap ($\mu < 0$) associated with hydrostatic compression (see Figure 1). Thus negative values of μ are to be expected for compacting rock, though in this case, the identification of the slope of the yield surface with a physical "friction coefficient" may not be appropriate. In Figure 1 the stress path for the standard axisymmetric compression test plots as a straight line with slope $\sqrt{3}$ intersecting the hydrostatic stress axis at the value of the initial confining stress. Therefore the paths for axisymmetric compression tests beginning at higher confining pressures intersect the cap closer to the mean stress axis. Presumably, values of μ more negative than those reported by *Olsson* [1999] for his confining pressures of 69 and 100 MPa would result for tests at higher confining pressures. This expectation was recently confirmed by Olsson in tests at confining pressures up to 250 MPa (W. A. Olsson, unpublished data, 1999). This evidence suggests that β and μ can be positive to very negative for high-porosity rock, depending on the stress state, and that band orientations that were previously rejected by RR (owing to extreme requirements on the values of β and μ) are feasible.

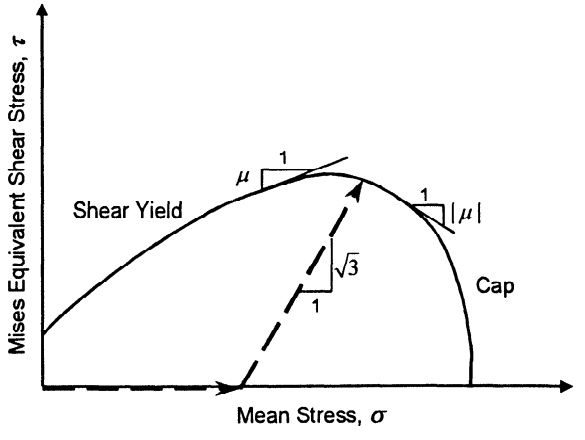

Figure 1. Schematic yield surface for porous sandstone. The onset of shear yield is represented by the diagonal line, while the cap is associated with compactive yield [*Olsson*, 1999]. The slope of the yield surface μ is positive for shear yield and negative for compactive yield. The dashed line represents an axisymmetric compression loading path.

The RR constitutive relation assumes all inelastic volume strain, either dilation or compaction, results from inelastic shearing and hence does not include inelastic compaction due to hydrostatic compression. Recognizing this, *Aydin and Johnson* [1983] added a term to (8) of the form $-d\sigma/k$, where k is an inelastic bulk modulus. The effect of this change is to replace the elastic bulk modulus K in (7) by an effective value $K^* = Kk/(K + k)$, which is slope of the mean stress-volume strain curve. We note, however, that the terms $-d\sigma/k$ and $\beta d^p\gamma$ will not, in general, both be active depending on the location of the current stress on the yield surface and the direction of the stress increment. For example, for the two-surface model depicted in Figure 1, $d^p\varepsilon = \beta d^p\gamma$ when the stress is on the shear yield surface and $d\tau > \mu d\sigma$, and $d^p\varepsilon = -d\sigma/k$ when the stress is on the cap and $d\sigma > 0$.

The effect of this additional term can also be included in the localization condition by replacing K by K^* in (9). In section 5, we show that this simple change can significantly decrease the magnitude of the hardening modulus required for localization.

4. Conditions for Band Formation

When the modulus tensor (9) of *Rudnicki and Rice* [1975] is substituted into (5) and the equation is solved for the hardening modulus h the result is

$$h = \frac{(Gn_iN_{ij}n_j + \beta K)(Gn_kN_{kl}n_l + \mu K)}{(\frac{4}{3}G + K)} + G\left[(n_iN_{ij}n_kN_{kj}) - (n_iN_{ij}n_j)^2\right] - (G + \mu\beta K). \quad (10)$$

Since h varies with the orientation of the potential plane of localization and generally decreases with ongoing inelastic deformation, RR argued that the orientation for which the localization criterion is first satisfied is that which yields the maximum value of h. To find this value, RR expressed (10) relative to the principal stress axes and determined the stationary values of h with respect to the components of the band normal n_i. The condition that the sum of squares of the n_i be one was implemented by the method of Lagrange multipliers. Which of the stationary values was actually maximum was determined by direct comparison of the resulting expressions for h. RR describe this procedure briefly in their appendix. Although they identified the possibility of a band of localized deformation perpendicular to one of the principal axes, corresponding to a compaction band, RR dismissed it because it required large magnitudes of β and μ that were inconsistent with data for the low-porosity rock-types. However, as noted in section 3, large negative values of β and μ are expected for high-porosity compacting rocks. Further-

more, *Perrin and Leblond* [1993] have corrected the range of β and μ for which the expression for the critical hardening modulus given by RR applies and the form of the critical hardening modulus for values of β and μ outside this range. These errors are of no consequence for the small values of β and μ appropriate for low porosity dilating rock but are pertinent to the possibility of compaction band formation. Consequently, here we expand the derivation in the appendix of RR emphasizing the possibilities for compaction band formation, and incorporating the corrections of *Perrin and Leblond* [1993].

The corrections given by *Perrin and Leblond* [1993] can also be extracted from the results given by *Ottosen and Runesson* [1991] for a more general class of constitutive relations that contains the RR form as a special case. *Ottosen and Runesson* [1991] did not, however, make explicit connection to the results of RR and did not discuss the relevance of the compaction band formation in terms of material parameters.

Expressing (10) relative to the principal axes of stress, including the constraint that the sum of squares of the n_i be one via a Lagrange multiplier λ, and finding the stationary values of the resulting expression with respect to the n_i yields

$$n_K N_K (N_K + \chi) = \lambda n_K, \text{ no sum on } K, \qquad (11)$$

where

$$\chi = \frac{1}{(1-\nu)} \left[\frac{1}{3}(\beta+\mu)(1+\nu) - \sum_{K=I,II,III} n_K N_K n_K \right], \qquad (12)$$

$N_K = s_K/\bar{\tau}$, s_K are the principal deviatoric stresses, and ν is Poisson's ratio. There are three possibilities: none, one, or two of the n_K are zero.

Although RR state that no solution is possible if none of the n_K are zero, there is, in fact, a solution but only if the stress state is purely hydrostatic (all N_K are zero). The corresponding critical hardening modulus is $-G\{1 + 4\beta\mu(1+\nu)/[9(1-\nu)]\}$, a value so negative as to be unlikely to be achieved in practice.

If one of the n_K is zero, then the maximum hardening modulus is given by $n_{II} = 0$. Thus the plane of the band contains the direction of the intermediate principal stress and the expression for the critical hardening modulus is that derived by RR:

$$\frac{h_{cr}}{G} = \frac{1+\nu}{9(1-\nu)}(\beta-\mu)^2 - \frac{1+\nu}{2}\left[N + \frac{1}{3}(\beta+\mu)\right]^2, \qquad (13)$$

where $N = N_{II} = s_{II}/\bar{\tau}$. (As discussed by RR, this expression neglects additional terms of order $\bar{\tau}/G$ which arise from the use of the Jaumann corotational stressrate in (3).) The prediction for the angle between the band normal and the least (most compressive) principal stress is given by RR but can be expressed in the following more illuminating form [*Rudnicki and Olsson*, 1998]:

$$\theta = \frac{\pi}{4} + \frac{1}{2}\arcsin\alpha, \qquad (14)$$

where

$$\alpha = \frac{(2/3)(1+\nu)(\beta+\mu) - N(1-2\nu)}{\sqrt{4-3N^2}}. \qquad (15)$$

This solution is valid for

$$\begin{aligned} (1-2\nu)N - \sqrt{4-3N^2} &\le \frac{2}{3}(1+\nu)(\beta+\mu) \\ &\le (1-2\nu)N + \sqrt{4-3N^2}. \end{aligned} \qquad (16)$$

Perrin and Leblond [1993] show that this condition results from the requirements that $n_{\rm I}^2 \ge 0$ and $n_{\rm III}^2 \ge 0$, but it can also be obtained by requiring that the band angle in (14) be real or that α satisfy $-1 \le \alpha \le 1$. *Perrin and Leblond* [1993] discuss in detail the differences between (16) and the conditions given by RR. Furthermore, they show that when one of the $n_K = 0$, only solution (13) is appropriate: within the range (16), (13) gives the largest hardening modulus, and outside this range one of the inequalities $n_{\rm I}^2 \ge 0$ or $n_{\rm III}^2 \ge 0$ is violated.

If two of the $n_K = 0$, then the third equals unity and the band is perpendicular to the principal axis corresponding to this direction. The critical value of the hardening modulus, given by *Perrin and Leblond* [1993], is obtained by inserting these values of the n_K into (10). The largest value of h is obtained for bands perpendicular to the maximum (largest tensile) or minimum (largest compressive) principal stress depending on whether N is greater or less than $(K/G)(\beta+\mu)$. Where this range overlaps with values of $\beta+\mu$ satisfying (16), these values of h can be shown to be less than that given by (13). When the inequality (16) is violated, the band is perpendicular to the axis of the most compressive principal stress if the left inequality is violated and perpendicular to the axis of the most tensile principal stress if the right inequality is violated. In the former case, the critical hardening modulus is given by

$$\begin{aligned} \frac{h_{cr}^{\rm III}}{G} &= \frac{(1+\nu)}{9(1-\nu)}(\beta-\mu)^2 \\ &\quad - \frac{(1+\nu)}{(1-\nu)}\left[\frac{1}{2}N_{\rm III} - \frac{1}{3}(\beta+\mu)\right]^2 \\ &\quad - \left(1 - \frac{3}{4}N_{\rm III}^2\right) \end{aligned} \qquad (17)$$

and in the latter by the same expression with $N_{\rm I}$ replacing $N_{\rm III}$. As noted by *Perrin and Leblond* [1993], expressions (13) and (17) and the corresponding expression with $N_{\rm I}$ replacing $N_{\rm III}$ are continuous. That is, as the left side of (16) approaches an equality, the shear band angle approaches 0°,and the expressions for h_{cr}^K, (13) and (17), are equal. Thus the shear and compaction bands coalesce (similarly for a right side equality, with 90° bands).

The ranges of $\mu+\beta$ for which the various solutions are valid are summarized in Figure 2. The upper and lower inequalities of (16) are shown as a function of the deviatoric stress state parameter N multiplied by $\sqrt{3}$ (actual plot is for $\nu = 0.2$). In the central region where (16) is satisfied, shear bands furnish the largest critical value of the hardening modulus h given by (13). Below this region, the sum $\mu+\beta$ is

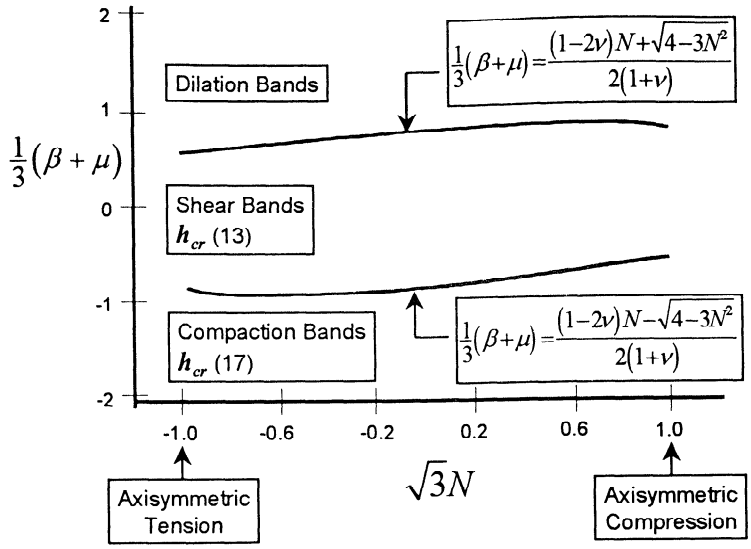

Figure 2. Predicted band orientation as functions of β (dilation coefficient) μ (slope of yield surface) and the deviatoric stress parameter, N (actual plot is for $\nu = 0.2$). The lines show the limiting equalities of equation (16).

less than the lower limit of (16): In this case, localization corresponds to compaction bands with the critical value of h given by (17). Above the central region, the sum $\mu + \beta$ exceeds the upper limit of (16), and bands (labeled "dilation bands" in Figure 2) are predicted to form perpendicular to the most tensile principal stress. Figure 3 gives another graphical representation of the solutions for axisymmetric compression. The values of β and μ where each of the three band orientations is predicted to occur and the regions where h_{cr} is positive are shown. Notice that the value of $(\beta + \mu)$ for a 40° shear band is expected to be significantly different than $(\beta + \mu)$ for a compaction band.

Since the latter two terms in (17) are negative, it is clear that h_{cr}^{III} can be positive only when $\beta \neq \mu$. This can also be seen graphically in Figure 3. Consequently, as for the shear bands (13), deviations from normality promote the possibility of localized deformation.

The expression for h_{cr}^{III} is quadratic in N_{III} with a minimum at $-(\mu+\beta)(1+\nu)/[3(1-2\nu)]$. The maximum value of h_{cr}^{III} occurs for axisymmetric compression, $N = N_{\mathrm{I}} = 1/\sqrt{3}$ and $N_{\mathrm{III}} = -2/\sqrt{3}$ if

$$(\mu + \beta) \leq 2\sqrt{3}(1 - 2\nu)/(1 + \nu), \tag{18}$$

which will be satisfied whenever β and μ are negative. In this case, (17) reduces to

$$\frac{h_{cr}^{\mathrm{III}}}{G} = -\frac{(1+\nu)}{3(1-\nu)}\left(1+\frac{2}{\sqrt{3}}\mu\right)\left(1+\frac{2}{\sqrt{3}}\beta\right). \tag{19}$$

Clearly, (19) demonstrates that compaction bands are predicted to occur with positive h only when $\mu < -\sqrt{3}/2$ or $\beta < -\sqrt{3}/2$ but not both (see Figure 3). For axisymmetric compression, (16) reduces to

$$-\sqrt{3} \leq \beta + \mu \leq \sqrt{3}\frac{(2-\nu)}{(1+\nu)}. \tag{20}$$

Thus compaction bands are predicted to occur when $\beta+\mu \leq -\sqrt{3}$ and the critical hardening modulus is given by (19). Note that even the most negative values reported by *Olsson* [1999] do not meet this condition. Nevertheless, it is clear that if the yield surface has a cap, β and μ can be sufficiently negative. Furthermore, because *Olsson* [1999] used (13) and (14) to evaluate the possibility of localization, he found that compaction bands were only possible at the lower limit of (20) for axisymmetric compression and at (16) in general. Here we have demonstrated that compaction bands are possible for a range of negative values of β and μ that appear to be representative of compacting rock (although data are scarce).

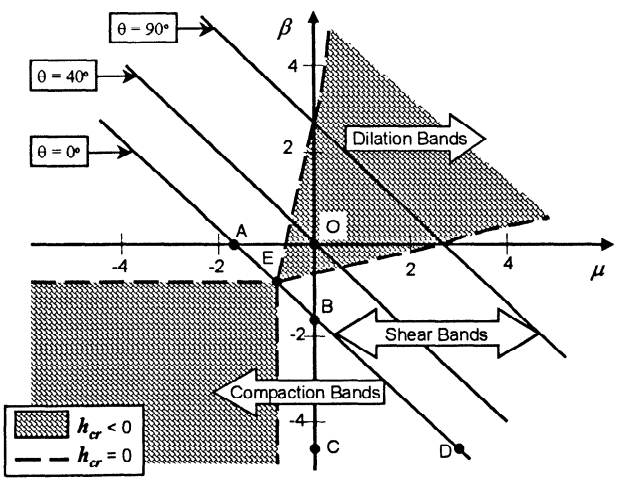

Figure 3. Predicted band orientations as functions of β and μ for axisymmetric compression (actual plot is for $\nu = 0.2$). Compaction bands ($\theta = 0°$) are predicted when $\beta + \mu \leq -\sqrt{3}$, while shear bands ($0° \leq \theta \leq 90°$) are predicted when $-\sqrt{3} \leq \beta + \mu \leq \sqrt{3}[(2-\nu)/(1+\nu)]$. The hatched areas denote a negative critical hardening modulus. Point E is located at $(-\sqrt{3}/2, -\sqrt{3}/2)$.

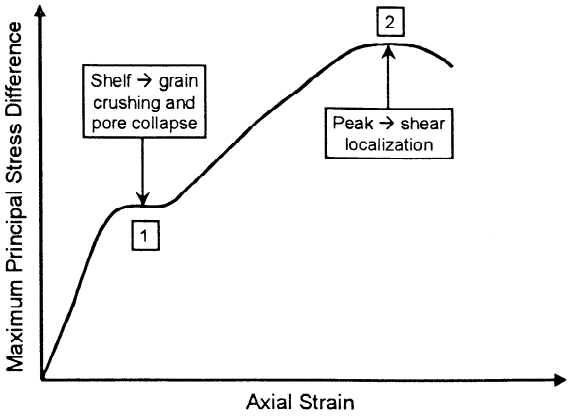

Figure 4. Schematic stress - strain curve for porous sandstone in axisymmetric compression. The shelf, (point 1), corresponds to grain crushing and pore collapse [*Zhang et al.*, 1990], while the peak, (point 2), is associated with shear failure [*Olsson*, 1999].

5. Discussion

A representative stress-strain curve (maximum principal stress difference versus axial strain) for a porous material loaded in axisymmetric compression is shown schematically in Figure 4. According to *Olsson* [1999] and *Wong et al.* [1992] the shelf is associated with pore collapse (see Figure 4, point 1) and the peak is associated with shear failure (Figure 4, point 2). The shape of this curve is consistent with an axisymmetric compression stress path (beginning at a sufficiently high confining pressure) that intersects the yield surface cap (see Figure 5, point 1), then pushes the cap outward until the shear yield surface is reached (Figure 5, point 2). As discussed in section 3, the value of μ will be negative on the cap (see Figure 5) and if the plastic potential has a similarly shaped cap, then β will also be negative. As the stress difference increases, the values of μ and β will become less negative and, presumably, evolve toward positive values associated with the shear yield surface.

The slope of the stress-strain curve for axisymmetric compression $E_{\tan}$ is related to the parameters of the constitutive relation by [*Rudnicki*, 1984]

$$E_{\tan} = \left[\frac{1}{2G(1+\nu)} + \frac{1}{3h}\left(1-\frac{\beta}{\sqrt{3}}\right)\left(1-\frac{\mu}{\sqrt{3}}\right)\right]^{-1}. \tag{21}$$

Thus negative values of β and μ decrease $E_{\tan}$, and therefore the intersection of the stress path with the cap could correspond to the observed shelf. Since negative values of β and μ also are appropriate with compaction bands, this framework is consistent with formation of compaction bands on the shelf. Once a compaction band has formed, the specimen is no longer homogeneous, and an interpretation of shear band formation as a bifurcation from homogeneous deformation is not rigorous. Nevertheless, because compaction corresponds to an increase in density (and, possibly, a decrease in grain size), formation of a compaction band may be associated with hardening, unlike shear band formation which is typically associated with softening. Therefore formation of a compaction band may not cause subsequent deformation to be concentrated in the band. Thus it is possible that deformation may proceed in a relatively homogeneous fashion until approximately peak stress, where shear localization develops as the stress path intersects the shear envelope.

This discussion has emphasized the possibilities of compaction band formation when the stress path intersects the cap, $\mu < 0$, and shear band formation when the stress path intersects the shear envelope, $\mu > 0$, but there are others. Within the triangle AOB in Figure 3, shear bands are possible when the stress state is on the cap, $\mu, \beta < 0$. Within the open-ended triangle CBD, compaction bands are possible when $\mu > 0$, $\beta < 0$, possibly corresponding to the shear envelope or the intersection of the cap and envelope.

Very few experimental data regarding the formation of compaction bands are available. *Olsson* [1999] reports values of β and μ that fall within (20), the allowable range of $(\beta + \mu)$ for shear bands (which did occur in specimens). However, at higher confining pressures, the loading path should intersect the cap, presumably resulting in more negative values of μ, which would satisfy the compaction band condition, $(\beta + \mu) \leq -\sqrt{3}$. Additionally, as shown by the detailed application of the RR constitutive framework to Tennessee marble [*Holcomb and Rudnicki*, 2000], μ and β can vary considerably with deformation even for low porosity rock. Clearly, further experimental work is needed to determine the material parameters at the onset of localized compaction.

We now examine the effect of including the modification of the constitutive relation by *Aydin and Johnson* [1983] to accommodate inelastic compaction due to hydrostatic compression. As noted in section 3, this modification is accomplished by replacing the elastic bulk modulus K with an effective value K^*. The resulting changes in the localization conditions (13)-(20) are made more evident by expressing

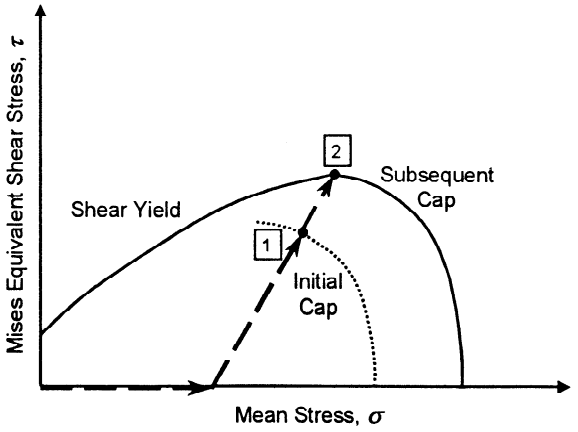

Figure 5. Schematic yield surface for porous sandstone, showing an axisymmetric compression stress path beginning at a high confining pressure. The yield surface cap is intersected first (point 1), and under continued loading, the cap is pushed outward until the shear yield surface is also intersected (point 2).

the change in terms of an effective Poisson's ratio ν^* defined by

$$\nu^* = \frac{3K^* - 2G}{2(3K^* + G)}. \quad (22)$$

Since the inelastic modulus k is likely to be much less than the elastic bulk modulus K, $K^* \simeq k$ and $K^* << G$, then $\nu^* \rightarrow -1.0$. As ν^* approaches -1.0, the critical value of the hardening moduli for shear bands, (13), approaches zero, while for compaction and dilation bands, $h^J_{cr}/G \rightarrow 3N_J^2/4 - 1$ (where J =I, III). For axisymmetric compression, $h^{\mathrm{III}}_{cr}/G \rightarrow 0$ (similarly, $h^{\mathrm{I}}_{cr}/G \rightarrow 0$ for axisymmetric tension). Thus inelastic compaction caused by mean stress tends to decrease the magnitude of the value of critical hardening modulus for which localized bands are predicted, allowing them to occur earlier in the program of deformation. Additionally, as $\nu^* \rightarrow -1$, the band angle degenerates: for axisymmetric compression, pure shear, and axisymmetric tension the band angles are required to be 0°, 45°, and 90°, respectively.

Porous sandstone under increasing hydrostatic pressure is characterized by a mean stress-volume strain curve which has an initial small nonlinear section, followed by a linear trend up to an inflection point, after which a period of grain crushing and pore collapse takes place, before hardening begins to occur (see Figure 6). It was previously suggested that compaction bands form on the shelf of the stress-strain curve, which corresponds to pore collapse and grain crushing. Therefore the slope (of the mean stress-volume strain curve) K^* during the pore collapse period can be used in (22) to determine the value of ν^* when compaction bands are believed to form. From a series of hydrostatic compression tests cited by *Olsson* [1999] (D. H. Zeuch unpublished data, 1996), the slope of the hydrostat during pore collapse/grain crushing is estimated as $K^* = 1.7$ GPa for Castlegate sandstone. Using $G = 8$ GPa, a value of $\nu^* = -0.4$ is found, while *Olsson* [1999] reports $\nu = 0.2$ for Castlegate sandstone. Some of the hydrostats from *Zhang et al.* [1990] for

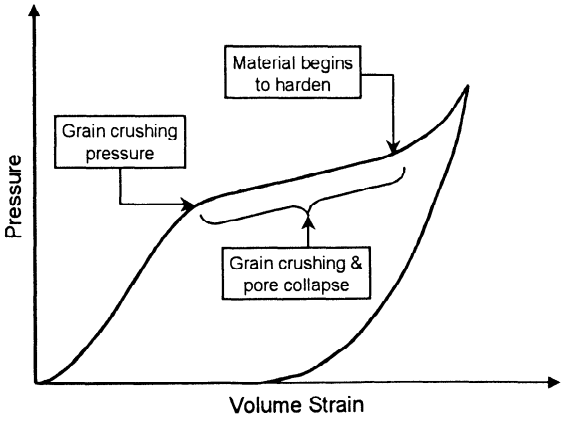

Figure 6. Schematic pressure - volume strain curve for porous sandstone. After the initial non-linear section, the curve is essentially linear up to the inflection point (grain crushing pressure), after which a period of grain crushing and pore collapse takes place, before the material begins to harden.

various sandstones include pore collapse/grain crushing sections with very small slopes, which would also correspond to fairly negative values for ν^*; certainly less than ν. Although these estimates of ν^* are rough, they demonstrate an important point. Including the effects of inelastic volume strain due to hydrostatic stress, results in a ν^* (at probable compaction band initiation) that is much less than the ν typically observed in porous sandstone. This causes the h^{III}_{cr} prediction using ν^* to be much closer to zero than that predicted using ν.

6. Conclusions

Compaction bands, thin zones of compressional deformation perpendicular to the direction of maximum compressive stress, have recently been observed in field and experimental specimens of high porosity sandstone. *Olsson* [1999] recognized that the shear localization theory of RR could be used to predict formation of compaction bands. Others (RR, [*Perrin and Leblond*, 1993]) previously identified this possible band orientation but discounted it because the required negative values for the material parameters β and μ (the dilatancy coefficient and the slope of the yield surface) were thought to be extreme. We have shown, however, that for materials (such as high-porosity sandstone) for which the inelastic volume strain is compactive and inelastic deformation is associated with stress states on a yield surface cap, strongly negative values are possible. *Olsson* [1999] suggested that the intersection of the stress path with the cap corresponds to the shelf often observed in the stress-strain curve of porous sandstone loaded in axisymmetric compression. Continued loading on this path pushes the cap out to the shear yield surface, eventually reaching peak stress.

The expressions for the critical hardening modulus (at the inception of localization) for both compaction and shear bands were presented. Either band type is possible, depending upon the stress path and confining pressure. Formation of a compaction band could result in material hardening, which may not preclude later shear localization. In both cases deviations from normality promote localization by increasing (making less negative) the critical hardening moduli. Inclusion of inelastic volume strain due to hydrostatic stress, as suggested by *Aydin and Johnson* [1983] tends to decrease the magnitude of the predicted h^{III}_{cr}, thus promoting compaction localization. Axisymmetric compression is the most favorable stress state for compaction band formation, requiring $\beta + \mu \leq -\sqrt{3}$. Although the limited data reported by *Olsson* [1999] do not satisfy this requirement, tests conducted at higher confining pressures should reveal μ to be significantly negative, thus satisfying $\beta + \mu \leq -\sqrt{3}$. Additional experimental work is needed to determine more precisely when compaction localization begins and to identify the corresponding material parameters.

Compaction bands are an important structure, since their reduced porosity and permeability could act as barriers to fluid flow in otherwise porous rock, thus impacting extraction or storage of fluids. Further work, both experimental and theoretical, is needed to understand and predict the for-

mation of compaction bands and their relation to localized shear bands.

Acknowledgments. Financial support for this work was provided by the U.S. Department of Energy,Office of Basic Energy Sciences, Geosciences Research Program through grantDE-FG02-93ER14344/09 to Northwestern University. We are grateful to W. A. Olsson and D. J. Holcomb for many helpful discussions and to W. A. Olsson for making his data available to us.

References

Aydin, A. and A.M. Johnson, Analysis of faulting in porous sandstones, *J. Struct. Geol., 5*, 10-31, 1983.

DiMaggio, F.L., and I. S. Sandler, Material model for granular Soils, *J. Eng. Mech. Div. Am. Soc. Civ. Eng., 97*, 935-950, 1971.

Hadamard, *J. Leçons sur la Propagation de Ondes et les Equations de L'Hydrodynamique*, A. Hermann, Paris, 1903.

Hill, R., Acceleration waves in solids, *J. Mech. Phys. Solids, 10*, 1-16, 1962.

Holcomb, D. J. and J. W. Rudnicki, Inelastic constitutive properties and shear localization in Tennessee marble, *Mech. Cohesive Frictional Mater.*, in press, 2000.

Mandel, J., Conditions de stabilté et postulat de Drucker, in *Rheology and Soil Mechanics*, edited by J. Kravtchenko and P. M . Sirieys pp. 58-68, Springer-Verlag, New York, 1966.

Mollema, P. N., and M. A. Antonellini, Compaction bands: A structural analog for anti-mode I cracks in aeolian sandstone, *Tectonophysics, 267*, 209-228, 1996.

Olsson, W.A., Theoretical and experimental investigation of compaction bands, *J. Geophys Res., 104*, 7219-7228, 1999.

Ottosen, N.S., and K. Runesson, Properties of discontinuous bifurcation solutions in elasto-plasticity, *Int. J. Solids Struct., 27*, 401-421, 1991.

Perrin, G., and J.B. Leblond, Rudnicki and Rice's analysis of strain localization revisited, *J. Appl. Mech., 60*, 842-846, 1993.

Rice, J. R., and J. W. Rudnicki, A note on some features of the theory of localization of deformation, *Int. J. Solids Struct., 16*, 597-605, 1980.

Rudnicki, J.W., A class of elastic-plastic constitutive laws for brittle rock, *J. Rheol., 28*, 759-778, 1984.

Rudnicki, J.W., and W.A. Olsson, Reexamination of fault angles predicted by shear localization theory, *Int. J. Rock Mech. Min. Sci., 35*, 4-5, 1998.

Rudnicki, J.W,. and J.R. Rice, Conditions for the localization of deformation in pressure-sensitive dilatant materials, *J. Mech. Phys. Solids, 23*, 371-394, 1975.

Thomas, T. Y., *Plastic Flow and Fracture in Solids*, Academic, San Diego, Calif., 1961.

Wong, T.-f., H. Szeto, and J. Zhang, Effect of loading path and porosity on the failure mode of porous rocks, *Appl. Mech. Rev., 45*, 281-293, 1992.

Wong, T.-f., C. David, and W. Zhu, The transition from brittle faulting to cataclastic flow in porous sandstones: Mechanical deformation, *J. Geophys. Res., 102*, 3009-3025, 1997.

Zhang, J., T.-F., Wong, and D. M. Davis, Micromechanics of pressure-induced grain crushing in porous rock, *J. Geophys. Res., 95*, 341-352, 1990

K. A. Issen, Department of Civil and Aeronautical Engineering, Clarkson University, Potsdam, NY 13699-5725

J. W. Rudnicki, Department of Civil Engineering, Northwestern University, Evanston, IL 60208-3109. (jwrudn@northwestern.edu)

(Received September 22, 1999; accepted May 18, 2000.)